Appl Nanosci (2016) 6:437–444
DOI 10.1007/s13204-015-0455-1

ORIGINAL ARTICLE

Facile approach to synthesize magnesium oxide nanoparticles by using *Clitoria ternatea*—characterization and in vitro antioxidant studies

N. John Sushma[1] · D. Prathyusha[1] · G. Swathi[1] · T. Madhavi[1] · B. Deva Prasad Raju[2] · K. Mallikarjuna[3] · Hak-Sung Kim[3]

Received: 14 March 2015 / Accepted: 27 April 2015 / Published online: 10 May 2015
© The Author(s) 2015. This article is published with open access at Springerlink.com

Abstract Facile approach to synthesize the metal oxide nanoparticles is getting an increased attention in various biomedical applications such as, to treat antibiotic resistant diseases. Magnesium oxide nanoparticles (MgO·NPs) were synthesized by using *Clitoria ternatea* as the stabilizer in a green synthesis approach. The preliminary screening of MgO·NPs in the presence of *C. ternatea* extract was observed by UV–visible spectrophotometer. X-ray diffraction (XRD) pattern have proved the crystalline nature of the MgO·NPs; Photoluminescence (PL) measurement studies are used to identify the quality and defects in the crystal structure. FE-SEM with EDS has showed the size of 50–400 nm with specific binding energies. FT-IR has revealed the functional groups present in the plant extract and the peak at 521 cm^{-1} indicated the characteristic absorption bands of MgO·NPs. The DPPH activity and reducing power assay of biologically synthesized MgO·NPs could reach 65 % at a concentration of 150 µg/ml, respectively. From the results it was concluded that the biologically synthesized MgO·NPs exhibit good antioxidant activity.

Keywords MgO nanoparticles · *Clitoria ternatea* · Antioxidant activity

✉ N. John Sushma
johnsushma@gmail.com

[1] Department of Biotechnology, Sri Padmavati Women's University, Tirupati 517502, India

[2] Department of Future Studies, Sri Venkateswara University, Tirupati 517502, India

[3] Department of Mechanical Engineering, Hanyang University, Seoul 133-791, South Korea

Introduction

Over the recent years, green nanotechnology have attracted considerable spouting research in many potential limelight fields of nanoscience and nanomedicine, which is dedicated for the creation, improvement and utility of nanostructures for advanced biomedical science. Due to their desired distribution, dispersion, sizes and shapes, the nanoparticles have numerous applications in human—day to day life, ranging from consumer goods to medicine (Mallikarjuna et al. 2015; Mahitha et al. 2015; Mansee Thakur et al. 2014). The main objective of this new field is to design and produce the multifunctional materials of nano scale range which are gearing the biological fields (Salata 2004; Nagarajan and Kuppusamy 2013) by making improvements in existing materials (Anamika Mubayi et al. 2012; Geoffrey Ozin and Cademartiri 2009; Revell 2006). The small and tiny particles consisting of large surface area is capable of protruding and reacting with various chemical groups to show their efficiency in various applications (Alivisatos and Barbara 1998). Production of nano scale materials can be done using eco-friendly biological synthesis which eliminates the use of chemicals that affect the environment (Brajesh Kumar et al. 2015). This has led to our current research interest in synthesizing the metal oxide nanoparticles using ethanolic extract of *Clitoria ternatea* that consists of bioactive functional elements which act as reducing and protecting agent in green chemistry.

Clitoria ternatea is a perennial climber commonly known as Aparajitha or Girikarnika which belongs to the family of Papillionacea. The morphological features (or) phenotypic characters appear as slender downy stems with leaves having multiple leaflets of elliptical shape and flowers of blue or white in colour are rich source of pharmacologically active secondary metabolites such as polyphenolic flavonoids,

anthocyanin glycosides, pentacyclic triterpenoids and phytosterols have been reported from this plant. Flavonols i.e., kaempherols, quercetin and myricetin and their glycosides used to treat body aches, infections, urinogenital disorders, as an anthelmentic and antidote to animal stings. *Clitoria ternatea* is commonly used as a brain tonic in Ayurvedic system of traditional Indian herbal medicine to ameliorate intelligence and intensify the memory function (Karuna Talpate et al. 2014), prevents convulsions as in epilepsy (anticonvulsant) and also as relaxing agent. Various activities of *C. ternatea* were reported as antioxidant, vascular smooth muscle relaxant and hepatoprotective agent (Mukherjee et al. 2007, 2008; Kuppan Nithianantham et al. 2011). Hence, in the present study, we have evaluated the ethanolic extract of *C. ternatea* was utilization in green nano MgO·NPs synthesis and their antioxidant activity. There are many metal oxides like MgO, ZnO, CaO, TiO_2 etc., which are known for their wide spread usage in diagnosing tools, remedy to treat illness and also as antimicrobial agents using in ointments due to their high catalytic activity (Vijayakumar et al. 2013).

Among various metal oxides, MgO is a functional semiconductor which has multiple applications in drug delivery (Seferos and Giljohann 2007), optoelectronics (Jackson et al. 2003), cell signalling and imaging (Parak et al. 2005) especially as successful potent antimicrobial and antioxidant agents fighting against most provocating antibiotic resistant dreadful diseases (Stoimenov et al. 2002; Nasibulin et al. 2009; Zhang et al. 2012). In the current study, we have employed the plant mediated production of MgO nanoparticles through calcination. This is a simple method among many methods like sol–gel combustion aerosol, laser vapourization, chemical gas phase deposition, hydrothermal techniques (Yu et al. 2004; Wang et al. 2008; Vandana Singh et al. 2015). In the process of size, shape, and crystalline nature of the MgO, nanoparticles are influenced by the parameters such as: temperature, pH and calcination time (Kenneth and Price 1999; Bhatte et al. 2011; Suslick et al. 1996). Hence, in this context, the authors made an attempt to synthesize the MgO·NPs using *C. ternatea* using variable parameters such as concentration of metal precursor, dosage of plant extract, pH and temperature, which were used to optimize the suitable condition for MgO·NPs preparation. The grown MgO·NPs were analysed by UV–visible spectroscopy, XRD, PL studies, FE-SEM, SEM, FT-IR, investigation of in vitro antioxidant activity by DPPH and reducing power assay.

Experimental

$MgCl_2·6H_2O$, NaOH, HCl and C_2H_5OH were of analytical grade chemicals (Merck and Himedia) and the plant was collected from Ramapuram village of Chittoor district, Andhra Pradesh, India. The *C. ternatea* plant is shown in Fig. 1.

The plant of *C. ternatea* was washed with running tap water and again thoroughly washed with double distilled water for several times and shade dried for about 7 days. Thoroughly dried whole plant was cut into pieces and made into fine powder. The fine powder of 5 g was taken in 100 ml of (70 % ethanol:30 % water) and stirred for 4 days. The extract was filtered through Whatman no 1 filter paper (pore size 20 µm) and supernatant was collected and stored at 4 °C for further nanoparticles synthesis process.

In biological synthesis of MgO·NPs fabrication, addition of ethanolic extract of *C. ternate* (reducing agent) to the aqueous $MgCl_2$ hexahydrate solution by adding NaOH drop wise under continuous stirring, at room temperature. The colour changed from green to yellowish colour. The solution generates $Mg(OH)_2$ which acts as precursor of MgO was centrifuged at 10,000 rpm for 10 min. The collected precipitation was washed with ethanol to remove impurities and formed pellet was calcinated at 100–300 °C, which gives the yellow powder form of MgO·NPs (Fig. 2).

The growing process of MgO nanoparticles using the plant extract was monitored after precipitate formation using double beam UV–visible spectrophotometer (GENESYS 10S UV–vis v4.002 2L9P112005) at a wavelength range of 200–800 nm. The crystalline phase formation and size of MgO·NPs were analysed using a PANalytical X'pert PRO X-ray diffractometer with CuK_α radiation ($\lambda = 0.154056$ nm) at 40 kV and 30 mA. The data was recorded over a 2θ range from 20° to 80° in the step scan mode with a step size of 0.02° at room temperature (RT).

Fig. 1 *Clitoria ternatea*

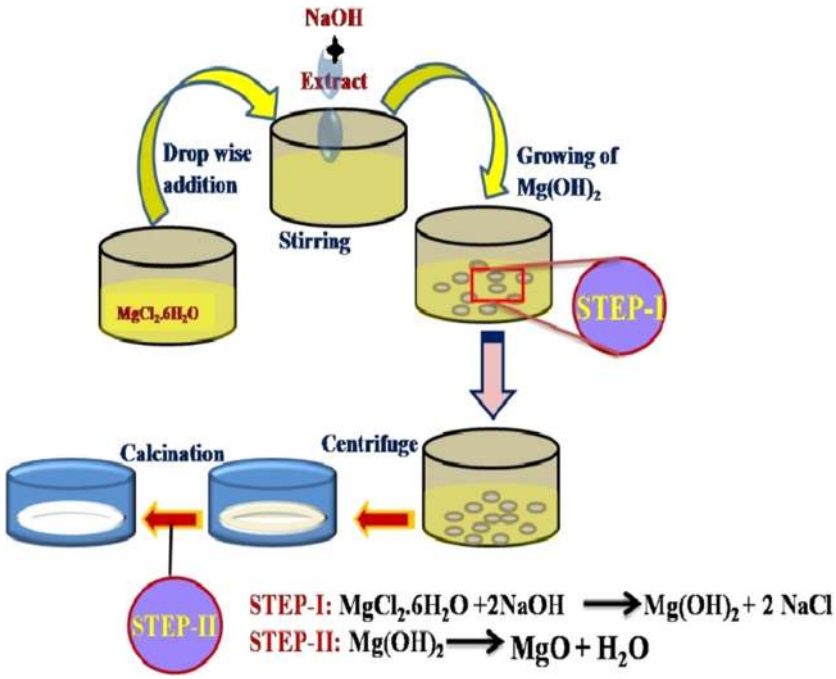

Fig. 2 Graphical image of biologically synthesized MgO nanoparticles

The photoluminescence spectra of biologically synthesized MgO·NPs measured in the 300–700 nm region were recorded with Jobin–yvon flurolog-3 spectrofluorometer using xenon flash lamp as light source at $\lambda em = 454$ nm, $\lambda ex = 380$ nm. The size and morphology of the MgO was investigated using a field emission scanning electron microscope (FE-SEM, Hitachi S-4200, Japan) and elemental analysis was carried out by energy dispersive X-ray analysis (EDS) which is attached to the FE-SEM X-ray column along with SEM images of biologically synthesized nanoparticles. Fourier transform infrared spectrum (FT-IR) of biologically synthesized MgO·NPs was recorded on Jasco FT-IR5300 model spectrophotometer using KBr pellets in the spectral range 4000–400 cm^{-1}. The antioxidant activity of MgO·NPs were tested using DPPH (1, 1-Diphenyl-2-picrylhydrazyl) and reducing power assay. All the measurements were carried out at room temperature (RT).

Antioxidant activity by DPPH assay

The sample containing hydrogen as a donor (A-H) when combined with DPPH gives strong absorbance at 517 nm where the colour change occurs from deep violet to pale yellow due to the acceptance of electron from MgO·NPs (antioxidant) by the DPPH. This results in the reduced form of DPPH-H, (i.e.) the transformation of free radical to non-radical form (Ilhami Gulcin et al. 2010). The reaction and the percentage (%) scavenging activity can be given as:

$$(\mathrm{DPPH}) + \mathrm{H-A} \rightarrow \mathrm{DPPH-H} + \mathrm{A}$$

$$\% \text{ scavenging} = [\text{Absorbance of control} - \text{Absorbance of test sample} / \text{Absorbance of control}] \times 100.$$

Reducing power assay

Reducing power acts as a reflection of antioxidant activity by the formation of different shades of bluish green colour based on the activity of the samples (Oktey et al. 2003). It is due to the presence of electron donors in the reducing assay compounds which can reduce the oxidized intermediates of lipid peroxidation process which acts as primary and secondary antioxidants. All the obtained results provide basic information that enables the further application of MgO·NPs in relevant fields.

Results and discussion

In plant mediated synthesis, the variable parameters such as dosage of *C. ternatea* extract, temperature and pH were measured with UV–visible spectrophotometer. Figure 3 suggests the sharp peak at 280 nm with increasing absorbance with different concentrations of plant extract indicates the nanoparticle formation from low concentration of the plant extract i.e. 200 µg, and size reduction was observed which may be due to the abundant availability of biomolecules in the plant extract. The results are in consonance with the previous report (Bar et al. 2009). Hence, the optimum concentration i.e. 200 µg was selected for further studies.

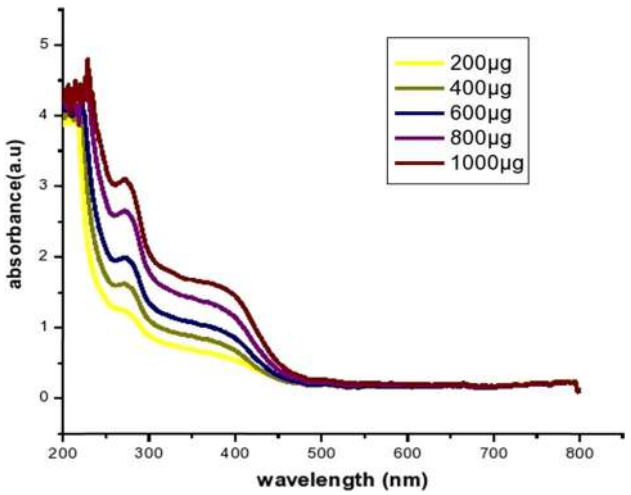

Fig. 3 UV–Vis spectra of biologically synthesized MgO·NPs

Temperature plays a crucial role during nucleation process of nanoparticle formation. $MgCl_2$ precipitation for the formation of MgO·NPs at specific temperatures is responsible for manipulating the particle size and morphology. The choice of precipitation temperature attributes to the changes between adsorption events of MgO·NPs and organic molecules used as surfactants or with ionic effects (Yildirim and Duncan 2012). In this spectroscopic analysis, the peak absorbance remained unaltered or nearly similar from 25 to 95 °C except at 45 °C as shown in Fig. 4, where the absorbance was increased. The current study indicates that 37 °C (RT) is the most favourable optimum temperature for MgO·NPs synthesis.

Effect of pH on the biological synthesis of MgO·NPs was tested by varying pH range from 10 to 12 as shown in Fig. 5 and at pH below 10, very little amount of precipitate formation is observed. From the UV–visible absorption spectra, it was clearly shown that the increase in absorbance at high pH (alkaline) leads to highly dispersed small sized nanoparticles with reduced aggregation due to presence of hydroxyl ions at high concentrations on the surface of nanoparticles. This is in consonance with the previous report (Ravichandran et al. 2011).

The wide angle XRD pattern clearly suggests the presence of cubic structure facets of MgO·NPs determined with diffraction peaks at 2θ values are 19(001), 33.1(100), 38.25(101), 50.93(102), 58.89(110), 62.25(220), 68.32(103), 72.22(111), 81(200), respectively. The sharpness of diffraction peaks indicates the crystalline nature of the plant extract reduced MgO·NPs and the obtained data was matched with reported JCPDS data card no: 002-1207 and is shown in Fig. 6. The average grain size 44 nm was calculated using Scherrer's formula (Balamurugan and Melba 2014).

Photoluminescence study is a very sensitive analysis to measure the quality of crystal structure, presence of oxygen vacancies as common defects and the emission mechanism was explained by Gaussian deconvolution based on emission spectrum. The PL emission spectrum of plant mediated nanocrystalline MgO·NPs powder as shown in Fig. 7 was recorded at 380 nm as an excitation wavelength with bandwidth equal to 5 nm and scanning rate equal to 200 nm/s. The PL emission spectrum reveals emission peak at blue region of 454 nm in 400–500 nm emission band range due to the donation of electrons to the conduction band by making holes in the valence band resulting in band to band excitation of MgO·NPs; this causes holes which migrate from the valence band to deep levels and recombination occurs between electrons from either the

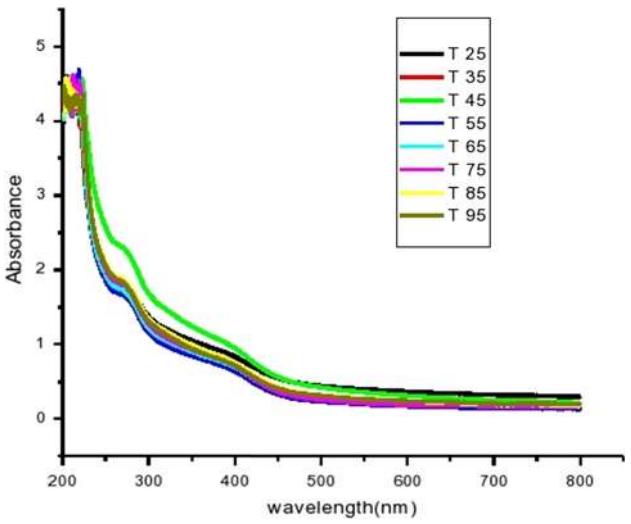

Fig. 4 UV–Vis spectra of temperature dependent MgO·NPs synthesis

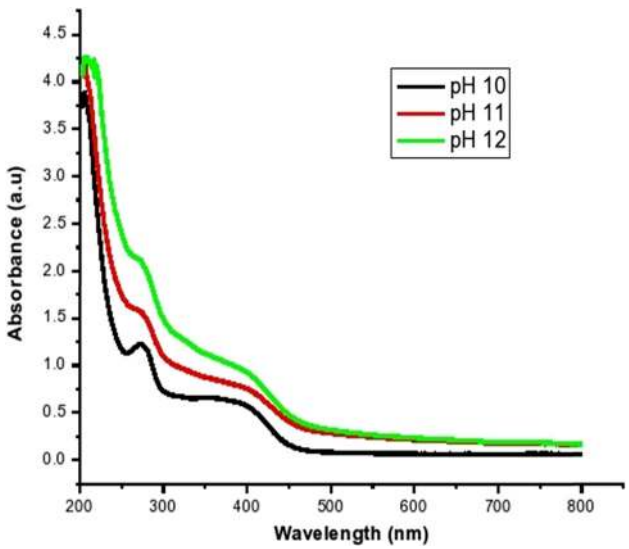

Fig. 5 UV–Vis spectra of pH dependent MgO·NPs synthesis

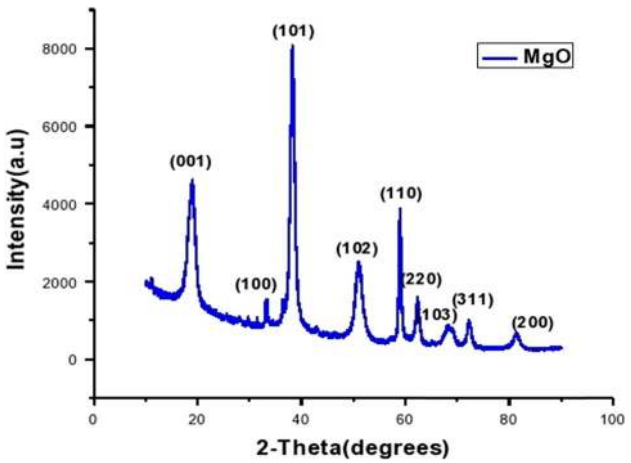

Fig. 6 XRD pattern of synthesized MgO·NPs

conduction band or shallow donor levels and trapped holes on deep levels (Kripal et al. 2011; Rao et al. 2012; Zeng et al. 2010).

The size, distribution and morphology of MgO·NPs were characterized by field emission scanning electron microscope (FE-SEM) and scanning electron microscopy (SEM). Figure 8a represents the typical FE-SEM image of biologically synthesized MgO·NPs. This represents well dispersed MgO·NPs, and the size range of 50 to 400 nm was observed. The elemental composition was revealed by energy dispersive X-ray spectroscopy (EDS) attachment with the FE-SEM instrument. In EDS spectrum, the peak positions at 0.261, 0.250, 0.245, 2.629 keV represents the binding energies of the magnesium as shown in Fig. 8b. SEM images of the synthesized samples at pH 10–12 as shown in Fig. 8c, and representing the dispersed nanoparticles of irregular shape with average size of 50–200 nm at pH 10 whereas pH 11 most of the particles were spherical as well as flat plate shaped with reduced average size of 50–100 nm among the dispersed particles. By further increasing the pH value from 10 to 12, the particles were slightly agglomerated with reduced size.

FT-IR spectroscopy was carried out to identify the functional groups present in the *C. ternatea* which acts as reducing and capping agents of synthesized MgO·NPs as shown in Fig. 9. The interaction of plant compounds with the chemical has shifted from weak to strong and broad peak at 3327 cm^{-1} due to water molecule, and medium peak was observed at 1637 cm^{-1} (–C = C–) stretch indicates the presence of alkenes and the peak observed at 521 cm^{-1} indicates the presence of MgO·NPs (Balamurugan et al. 2014).

Antioxidant activity of MgO·NPs

Free radical scavenging activity by Diphenylpicrylhydrazyl (DPPH) was assessed according to the method Blois (1958) with slight modification. Briefly, 50–150 µl (1 mg/ml) of crude extract of the plant was tested and compared with standard ascorbic acid. The plant showed the maximum antioxidant activity which is almost similar to standard. Powder form of MgO·NPs synthesized by biological forms were dissolved in distilled water and added to the 1 ml of 1 mM DPPH. The mixture was shaken well and incubated at room temperature for 30 min and absorbance was measured at 517 nm in a spectrophotometer. The experiment was performed in triplicate and average was taken

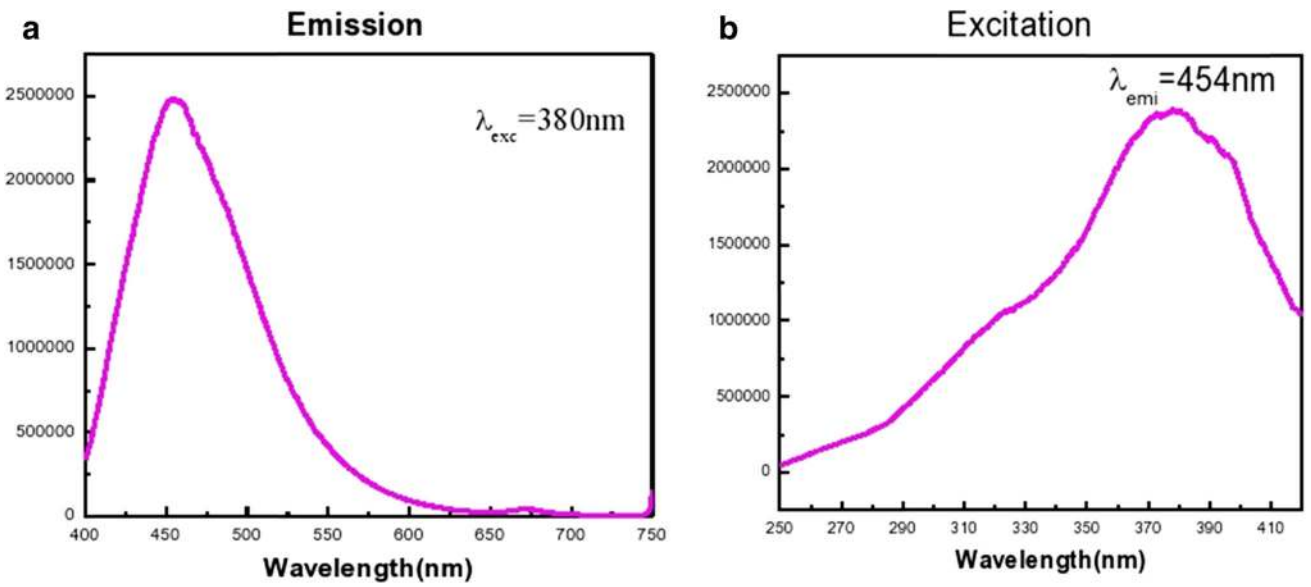

Fig. 7 **a** Emission spectrum of MgO·NPs at 454 nm, **b** excitation spectrum of MgO·NPs at 380 nm

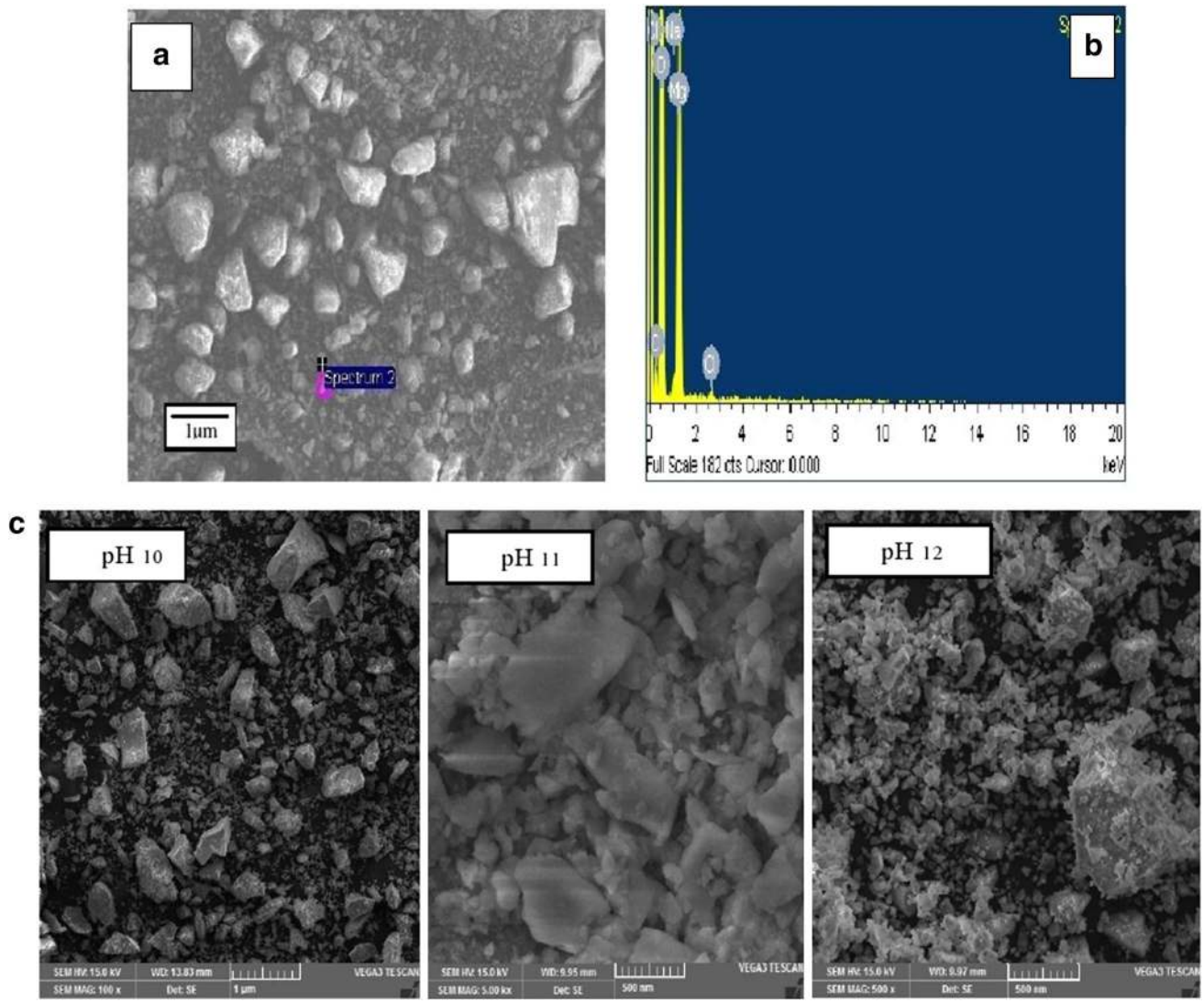

Fig. 8 **a** FE-SEM image and **b** energy dispersive X-ray fluorescence spectrometry—spectra of MgO·Nps synthesized by using *Clitoria ternatea*, **c** SEM images of biological samples at pH (10, 11, 12)

for determination of percentage inhibition. From Fig. 10, it was observed that the biologically synthesized MgO·NPs has 65 % maximum inhibition activity. This maximum inhibition of *C. ternatea* synthesized MgO·NPs may be due to the bioactive components present in the plant extract.

The reducing power of MgO·NPs was determined by following the method of Oyaizu (1986). Briefly, 50–150 µg (1 mg/ml) of biologically synthesized MgO·NPs was dissolved in distilled water and added to the 0.5 ml of 0.2 M phosphate buffer (pH 6.6) and 0.5 ml potassium ferrocyanide (1 %). After incubating the mixture at 50 °C for 20 min, 0.5 ml of 10 % trichloroacetic acid was added and then mixture was undisturbed for 15 min. In this assay, the yellow colour of test solution turns to different shades of blue and green depending on the reducing power of MgO·NPs. The colour developed was measured at 700 nm using UV–visible spectrophotometer. Figure 11 represents that plant synthesized MgO·NPs have reducing power.

Conclusion

In the present study by using *C. ternatea*, MgO·NPs were rapidly biosynthesized and it was confirmed by the initial colour change of light yellow which was obtained at optimized metal: plant concentration of 25 mM: 200 µg, temperature of 37 °C, pH of 12 and peak position at 280 nm observed by UV–visible spectrophotometer. The cubic shape of MgO·NPs was obtained by XRD analysis, PL intensity confirmed the quality and defects in the crystal

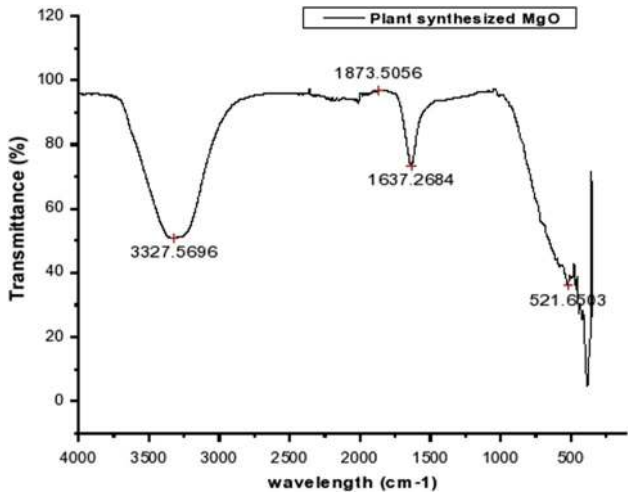

Fig. 9 FT-IR spectrum of MgO·NPs synthesized from *Clitoria ternatea* extract

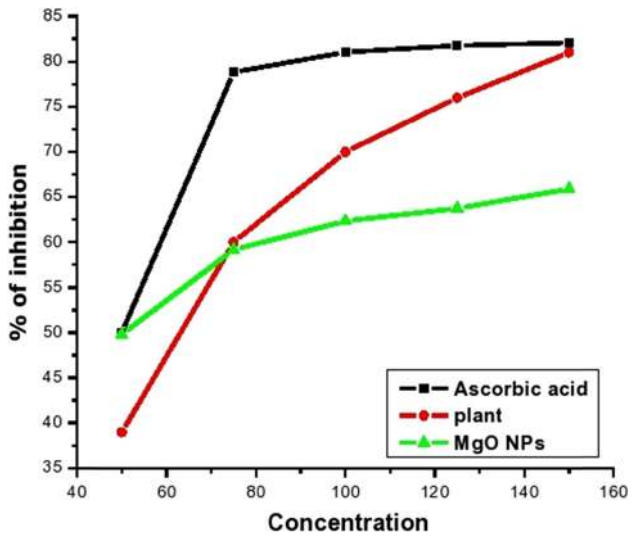

Fig. 10 Antioxidant activity of plant synthesized MgO·NPs by DPPH assay

structure, FE-SEM with EDS and SEM have showed the average size of 50–400 nm with specific binding energies. FT-IR has revealed the presence of functional groups in the plant extract, and spectra peak at 521 cm^{-1} indicated the characteristic absorption band of MgO·NPs. In vitro antioxidant activity of MgO·NPs by DPPH and reducing power assay has proved that biologically synthesized MgO·NPs have 65 % inhibition activity. The potential antioxidant activity of biologically synthesized MgO·NPs may be due to the presence of bioactive components of the plant extract. Hence, the biologically synthesized MgO·NPs have potential in vitro antioxidant activity, and further studies will be carried out to find in vivo antioxidant activity of MgO·NPs.

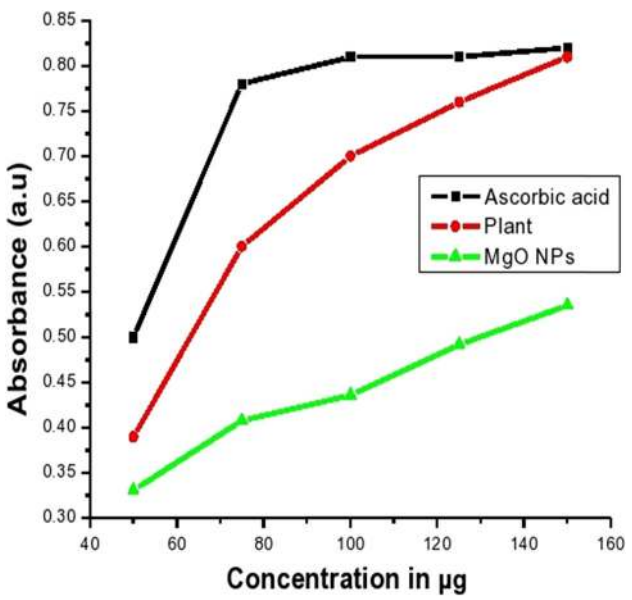

Fig. 11 Antioxidant activity of plant synthesized MgO·NPs by reducing power assay (ascorbic acid as reference)

Acknowledgments The corresponding author is highly grateful to DST-SERB, Department of Science and technology, Government of India, New Delhi, for sanctioning major research project vide reference number SB/EMEQ-341/2013, dated 17-10-2013.

Open Access This article is distributed under the terms of the Creative Commons Attribution 4.0 International License (http://creativecommons.org/licenses/by/4.0/), which permits unrestricted use, distribution, and reproduction in any medium, provided you give appropriate credit to the original author(s) and the source, provide a link to the Creative Commons license, and indicate if changes were made.

References

Alivisatos P, Barbara PF (1998) From molecules to materials: current trends and future directions. Adv Mater 10:1297–1336. doi:10.1007/978-94-015-9576-6-4

Balamurugan S, Melba K (2014) Nanomaterials prepared by ball milling, citrate sol gel, and molten salt flux methods. J Nano Sci Nano Tech 14:1–9. doi:10.1166/jnn.9770

Balamurugan S, Ashna L, Parthiban P (2014) Synthesis of nanocrystalline MgO particles by combustion followed by annealing method using hexamine as a fuel. J Nano Tech 6:1–6. doi:10.1155/2014/841803

Bar H, Bhui DH, Sahoo PG, Sarkar P, De PS, Misra A (2009) Green synthesis of silver nanoparticles using latex of *Jatropha curcas*. Colloid Surf A Physicochem Eng Asp 339:134–139. doi:10.1016/j.colsurfa.2009.02.008

Bhatte KD, Fujita S, Arai M, Pandit AB, Bhanage BM (2011) Ultrasound assisted additive free synthesis of nanocrystalline zinc oxide. Ultrason Sono chem 18:54–58. doi:10.1016/j.ultsonch.2010.06.001

Blois MS (1958) Antioxidant determinations by the use of a stable free radical. Natr 181:1199–1200. doi:10.1038/1811199a0

Geoffrey Ozin A, Cademartiri Ludovico (2009) Nanochemistry, what is next? Small 5:1240–1244. doi:10.1002/smll.200900113

Gulcin Ilhami, Huyut Zubeyr, Elmastaş Mahfuz, Hassan Aboul-Enein Y (2010) Radical scavenging and antioxidant activity of Tannic acid. Arabian J Chem 3:43–53. doi:10.1016/j.arabjc.2009.12.008

Jackson JB, Westcott SL, Hirsch LR, West JL, Halas NJ (2003) Controlling the surface enhanced raman effect via the nanoshell geometry. Appl J Phys Lett 82:257–259. doi:10.1063/1.1534916

Karuna Talpate A, Uma Bhosale A, Mandar Zambare R, Rahul Somani S (2014) Neuroprotective and nootropic activity of *Clitorea ternatea* linn. (fabaceae) leaves on diabetes induced cognitive decline in experimental animals. J Pharm Bioallied Sci 6:48–55. doi:10.4103/0975-7406.124317

Kenneth SS, Price G (1999) Application of ultrasound to materials chemistry. J Annu Rev Mater Sci 29:295–326. doi:10.1146/annurev.matsci.29.1.295

Kripal R, Gupta AK, Srivastava RK, Mishra SK (2011) Photoconductivity and photoluminescence of ZnO nanoparticles synthesized via co-precipitation method. Spectrochim Acta Part A 79:1605–1612. doi:10.1016/j.saa.2011.05.019

Kumar Brajesh, Smita Kumari, Cumbal Luis, Debut Alexils, Camacho Javier, Hernandez-Gallegos Elisabeth, de Guadalupe María, Chavez-Lopez Marcelo Grijalva, Angulo Yolanda, Rosero Gustavo (2015) Pomosynthesis and biological activity of silver nanoparticles using *Passiflora tripartita* fruit extracts. Adv Mater Lett 6:127–132. doi:10.5185/amlett.2015.5697

Mahitha B, Deva Prasad Raju B, Mallikarjuna K, Durga Mahalakshmi ChN, John Sushma N (2015) *Bacopa monniera* stabilized silver nanoparticles attenuates oxidative stress induced by aluminum in albino mice. J Nano Sci Nano Technol 15:2015. doi:10.1166/jnn.8995

Mallikarjuna K, Narasimha G, John Sushma N, Dillip GR, Subba Reddy BV, Sreedhar B, Deva Prasad Raju B (2015) Biogenic preparation of gold nanostructures reduced from *Piper longum* leaf broth and their electrochemical studies. J Nano Sci Nano Technol 15:1280–1286. doi:10.1166/jnn.2015.8889

Mubayi Anamika, Chatterji Sanjukta, Prashant MR, Watal Geeta (2012) Evidence based green synthesis of nanoparticles. Adv Mat Lett 3(6):519–525. doi:10.5185/amlett.2012.Icn-ano.353

Mukherjee PK, Kumar V, Houghton PJ (2007) Screening of Indian medicinal plants for acetylcholinesterase inhibitory activity. Phyto Ther Res 21:1142–1145. doi:10.1002/ptr.2224

Mukherjee PK, Kumar V, Kumar NS, Heinrich M (2008) The ayurvedic medicine *Clitoria ternatea*—from traditional use to scientific assessment. J Ethnopharmacol 120:291–301. doi:10.1016/j.jep.2008.09.009

Nagarajan Sangeetha, Kuppusamy Kumaraguru Arumugam (2013) Extracellular synthesis of Zinc Oxide nanoparticle using seaweeds of gulf of mannar. India J Nano Biotech 11:39. doi:10.1186/1477-3155-11-39

Nasibulin AG, Sun L, HaaMaaLaInen S, Shandakov SD, Banhart F, Kauppinen EI (2009) In situ TEM observation of MgO nanorod growth. J Cryst Growth Des. doi:10.1021/cg9010168

Nithianantham Kuppan, Shyamala Murugesan, Chen Yeng, YogaLatha Lachimanan, Subramanion L, Jothy Sreenivasan Sasidharan (2011) Hepatoprotective potential of *Clitoria ternatea* leaf extract against paracetamol induced damage in mice. Mol 16:10134–10145. doi:10.3390/molecules161210134

Oktey M, Gulcin I, Kufrevioglu OI (2003) Determination of in vitro antioxidant activity of fennel (*Foeniculum vulgare*) seed extracts. Lebensum Wisss U Technol 36:263–271. doi:10.1016/S0023-6438(02)00226-8

Oyaizu M (1986) Studies on product of browning reaction prepared from glucose amine. Jpn J Nut 44:307–315 **ISSN: 0021-514**

Parak WJ, Pellegrino T, Plank C (2005) Labelling of cells with quantum dots. Nano Technol 16:9–25. doi:10.1088/0957-4484/16/2/R01

Rao TP, Kumar MCS, Hussain NS (2012) Effects of thickness and atmospheric annealing on structural, electrical 300 and optical properties of GZO thin films by spray pyrolysis. J Alloy Compds 541:495–504. doi:10.1016/j.jallcom.2012.05.128

Ravichandran V, Tiah ZX, Subashini G, Terence FWX, Eddy FCY, Nelson J, Sokkalingam AD (2011) Biosynthesis of silver nanoparticles using *Mangosteen* leaf extract and evaluation of their antimicrobial activities. J Saudi Chem Soc 15:113–120. doi:10.1016/j.jscs.2010.06.004

Salata OV (2004) Applications of nanoparticles in biology and medicine. J Nano Biotech 2:3–8. doi:10.1186/1477-3155-2-3

Seferos DS, Giljohann DA (2007) Nano-flares—probes for transfection and mRNA detection in living cells. J Am Chem Soc 129:15477–15479. doi:10.1021/nn9003814

Singh Vandana, Tiwari Stuti, Pandey Sadanand, Preeti Rashmi Sanghi (2015) *Cassia Grandis* seed Gum-*graft*-poly(acrylamide)-silica hybrid: an excellent Cadmium (ii) adsorbent. Adv Mater Lett 6:19–26. doi:10.5185/amlett.2015.5603

Stoimenov PK, Klinger RL, Marchin GL, Klabunde KJ (2002) Metal oxide nanoparticles as bactericidal agents. Langmuir 18:6679–6686. doi:10.1021/la0202374

Suslick KS, Hyeon T, Fang M (1996) Nanostructured materials generated by high- intensity ultrasound—sonochemical synthesis and catalytic studies. Chem Mater 8:2172–2179. doi:10.1021/cm960056l

Thakur Mansee, Gupta Himanshu, Singh Dipty, Ipseeta Mohanty R, Maheswari Ujjwala, Vanage Geeta, Joshi DS (2014) Histopathological and ultrastructural effects of nanoparticles on rat testis following 90 days (chronic study) of repeated oral administration. J Nano Biotech 12:42. doi:10.1186/s12951-014-0042-8

Vijayakumar M, Priya K, Nancy FT, Noorlidah A, Ahmed ABA (2013) Biosynthesis, characterisation and anti-bacterial effect of plant-mediated silver nanoparticles using *Artemisia nilagirica*. Indust Crops Prod 41:235–240. doi:10.1016/j.indcrop.2012.04.017

Wang G, Zhang L, Dai H, Deng J, Liu C, He H, Au CT (2008) Assisted hydrothermal synthesis and characterization of rectangular parallelepiped and hexagonal prism single-crystalline MgO with three-dimensional worm hole like mesopores. Inorg Chem 47:4015–4022. doi:10.1021/ic7015462

Yildirim OA, Duncan C (2012) Effect of precipitation temperature and organic additives on size and morphology of ZnO nanoparticles. J Mater Res 27:1452–1461. doi:10.1557/JMR.2012.58

Yu JC, Xu A, Zhang L, Song R, Wu L (2004) Synthesis and characterization of porous magnesium hydroxide and Oxide nanoplates. J Phys Chem B 108:64–70. doi:10.3390/s100504855

Zeng H, Duan G, Li Y, Yang SK, Xu X, Cai W (2010) Blue luminescence of ZnO nanoparticles based on non-equilibrium processes—defect origins and emission controls. Adv Funct Mater 20:561. doi:10.1002/adfm.200901884

Zhang YG, He HY, Pan BC (2012) Structural features and electronic properties of MgO nanosheets and nanobelts. J Phys Chem C 116:23130–23135. doi:10.1021/jp3077062